Effects of As and Mn doping on microstructure and electrical conduction in ZnO films

K. Lord, T. M. Williams, D. Hunter, K. Zhang, J. Dadson, and A. K. Pradhan[a)]
Center for Materials Research, Norfolk State University, 700 Park Avenue, Norfolk, Virginia 23504

(Received 6 March 2006; accepted 11 May 2006; published online 29 June 2006)

We report the synthesis of epitaxial As-doped ZnO and Mn-doped (ZnAs)O films by pulsed-laser deposition technique. The grain size in (ZnAs)O films decreases from 40 to less than 10 nm upon Mn doping, illustrating that Mn acts as a potential catalyst to create nanosize grains. Temperature dependent electrical resistance shows metal-insulator transition and metal-semiconductor transition (MST) at 165 and 115 K, respectively, in (ZnAs)O, although Mn doping suppresses MST completely. Both ionization efficiency on oxygen vacancies and percolation of charge carriers may be responsible for such transitions. In addition, electrical conduction in these films shows strong aging effects. © *2006 American Institute of Physics*. [DOI: 10.1063/1.2217257]

Two important characteristics, such as direct wide band gap (3.37 eV) and large exciton binding energy (60 meV), make ZnO a promising material for short wavelength, low-power consuming light-emitting and laser diodes.[1] The importance of *p*-type doping in ZnO remains a clue to realize potential applications as UV light emitters, transparent high-power electronics, piezoelectric transducers, and chemical and gas sensors for ZnO. However, ZnO is inherently prone to becoming an *n*-type semiconductor, so it has been difficult to manufacture high-repeatability *p*-type semiconductors. It is apparent from recent reports[2–7] that fabricating *p*-type ZnO semiconductor posed an extremely stiff challenge. Although phosphorus and arsenic have been considered as *p*-type dopants, they are found not to be reliable, while nitrogen incorporation has proven to be a suitable acceptor for making ZnO films *p*-type. Recently, it has been reported that As doping in ZnO film synthesized by pulsed-laser deposition (PLD) technique showed *p*-type carrier conduction.[8] However, doping with group V elements in ZnO has not been reliable.

The metal-insulator transition is generally explained by the increase in carrier concentration and formation of a degenerate band due to doping, as predicted by Mott.[9] However, extrinsic as well as intrinsic donors are known to affect the carrier concentration and the conductivity, the nature and interdependence of these entities is far from understood. In this letter, we report on the growth of epitaxial ZnO:As and Mn-doped ZnO:As films by the pulsed-laser deposition (PLD) technique in order to understand the effect of doping and codoping in ZnO. It is demonstrated that Mn doping in ZnO:As films yields drastic reduction of the grain size, illustrating that Mn acts as a catalyst in this system to create nanosize grains. Temperature dependent electrical resistance shows two transitions: a metal-insulator transition (MIT) and a metal-semiconductor transition (MST) at 165 and 115 K, respectively, in (ZnAs)O. However, doping with Mn suppresses MST completely, although a weak peak is seen for MIT. It is believed that ionization efficiency on oxygen vacancies[10] and percolation of charge carriers in two competing phenomena may be responsible for such transitions.

Doped ZnO epitaxial films were grown on sapphire/(0001) substrates by the PLD technique (KrF excimer, $\lambda=248$ nm, laser repetition rate of 5 Hz) with a pulse energy density of $1-2$ J/cm^2. High-density As-doped ZnO target was synthesized by mixing a stoichiometric amount of ZnO and 1 mol % Zn_2As_3 (both 99.99% purity) powders, calcining at 400 °C for 12 h followed by isostatic pressing at 400 MPa, and finally sintering at 500 °C. For Mn doping, 5 at. % MnO_2 (99.99% purity) powders were mixed with As-doped ZnO calcined powders with further calcining at 400 °C for 12 h followed by isostatic pressing at 400 MPa, and finally sintering at 500 °C. It is noted that As was introduced into ZnO first in order to avoid any alloying of Mn with As. Clean single crystalline sapphire substrates were loaded to the chamber and heated just after the ultimate base pressure $<3\times10^{-8}$ Torr is reached. The films of about 300 nm thickness were deposited at a substrate temperature $T_s=500-600$ °C at oxygen partial pressure $PO_2=1-50$ mTorr. *In situ* annealing at 200 °C was performed in 400 Torr of nitrogen for 3 min just after the film was deposited. Rapid thermal annealing in nitrogen was also carried out on some films. The x-ray diffraction (XRD) of the films was done in a Rigaku x-ray diffractometer using Cu $K\alpha$ radiation. Surface microstructure of the films was analyzed by atomic force microscopy (AFM). Temperature dependence of electrical conductivity and current-voltage (*I-V*) characteristics were measured by a semiconductor parameter analyzer using four-probe technique. Either In or In/Au contact pads were used. The samples were also annealed in nitrogen at 200 °C using rapid thermal annealing process after making evaporated contact pads.

Figure 1 shows typical XRD patterns recorded for both As-doped ZnO and (ZnAs)MnO films grown at 600 and 500 °C, respectively. Only the Bragg reflections that correspond to the ZnO (002) and (004) planes appear along with the Al_2O_3 substrate (006) reflection, indicating that the film was *c*-axis oriented. Absence of any other peak illustrates that the films are single phase. The full width at half maximum (FWHM) for (002) increases from 0.27° for As-doped ZnO to 0.42° for (ZnAs)MnO. The rocking curves for both films are shown in the inset of Fig. 1 in order to elucidate the increase in FWHM on Mn doping. The FWHM also describes the qualitative crystalline behavior of the film. The

[a)]Electronic mail: apradhan@nsu.edu

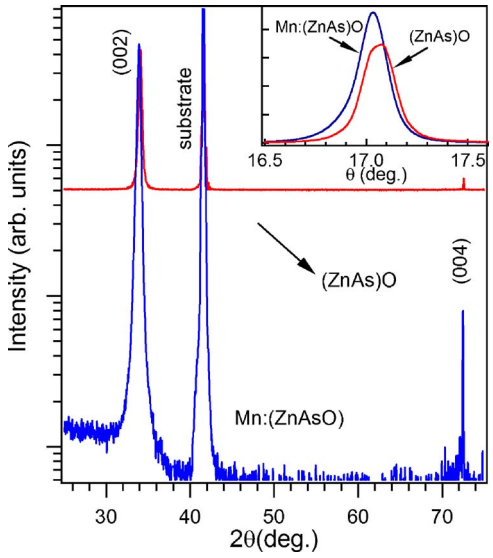

FIG. 1. (Color online) XRD patterns of the (ZnAs)O and (ZnAs)MnO films. The inset shows the rocking curves for both films.

(002) peak in (ZnAs)MnO shifts to lower angle compared to As-doped ZnO film. This indicates that Mn (1.79 Å) has substituted Zn (1.53 Å) sublattice due to their closer size of the atomic radius. However, it is unlikely for Mn to substitute As due very small atomic radius of As (1.33 Å), where as it is obvious for the case substitution of As into the Zn site.

AFM results are presented in Figs. 2(a) and 2(b) for (ZnAs)O and (ZnAs)MnO, respectively, in order to visualize the effects of Mn doping on grain size of the film and the consequent surface roughness. It is very clear that both films are quite dense and contain very smooth surface roughness with uniform grain size. However, the grain size in (ZnAs)MnO is less than 10 nm compared to 40 nm in (ZnAs)O film. On the other hand, the surface roughness reduces from 1 to 0.8 nm on Mn doping, illustrating the smoother surface in (ZnAs)MnO film. In order to gain a clear picture on surface roughness and quality, three-dimensional (3D) AFM images of (ZnAs)O and (ZnAs)MnO are shown in Figs. 3(a) and 3(b), respectively. The AFM images clearly show surface morphology consisting of individual grains, well-defined size, and extent of surface roughness as described above. The XRD results along with AFM microstructure of the films clearly show that the films are highly crystalline.

Figure 3 shows the temperature dependence of the normalized electrical resistivity of (ZnAs)O and (ZnAs)MnO films. The (ZnAs)O film shows a pronounced MIT at 165 K and semiconducting behavior at temperatures above it. However, the same film shows a MST at 115 K, as can be clearly seen in the inset. The film showed negative temperature coefficient of resistance (TCR) above MIT, which is a characteristic of a semiconducting behavior. The positive TCR metal-type conductivity behavior observed below MIT can be explained by the formation of a degenerate band appearing in heavily doped semiconductors as suggested by Mott.[9] This type of MST transition was seen in Ga:ZnO,[10] Nb:TiO_2,[11] and Al:ZnO (Ref. 12) semiconductors. However, MST completely disappears with Mn doping into (ZnAs)O leaving behind a small MIT transition in the temperature dependent resistivity, as shown in Fig. 3. It was argued that

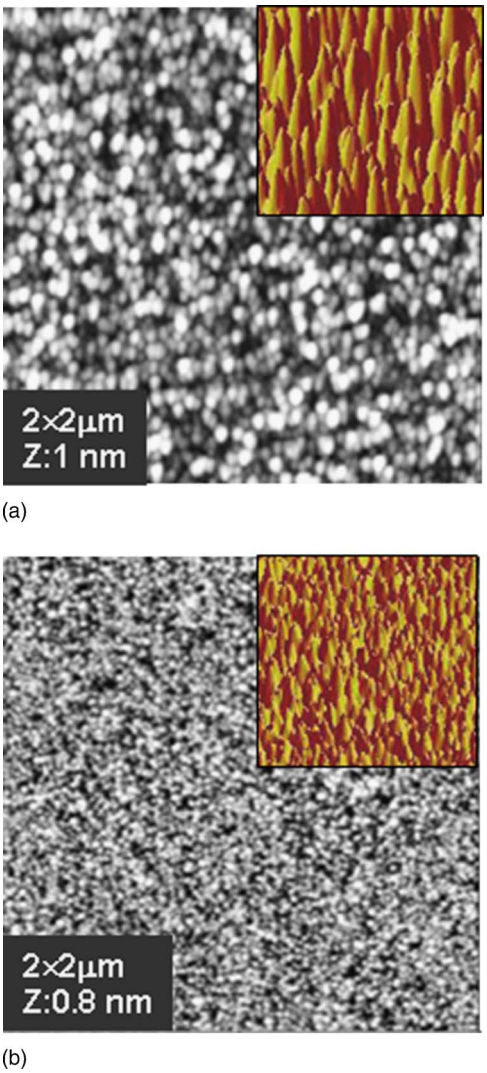

FIG. 2. (Color online) AFM images of (a) (ZnAs)O and (b) (ZnAs)MnO films. The corresponding 3D images of both films over a same area are shown in respective insets.

both dopant addition and its effect on ionization efficiency on oxygen vacancies may be responsible for the MST transition found in highly conducting Ga:ZnO (Ref. 10) semiconductor. In that context, ionization efficiency on oxygen

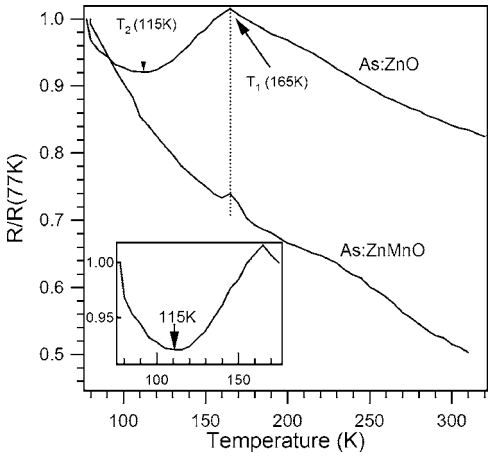

FIG. 3. (Color online) Plot of normalized resistivity vs temperature for (ZnAs)O and (ZnAs)MnO films, indicating transitions. The inset shows the enlarged view of the MST transition.

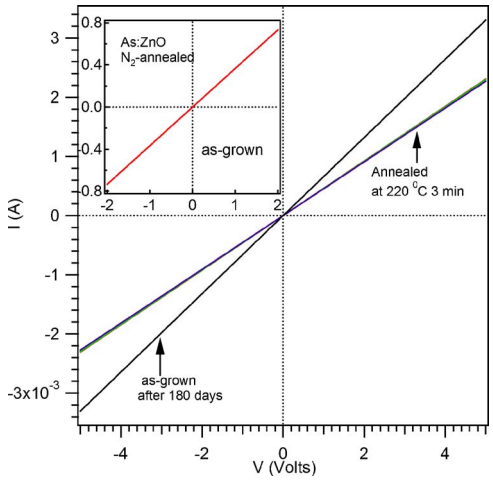

FIG. 4. (Color online) *I-V* characteristics for (ZnAs)O films with rapid thermal annealing in nitrogen measured after 180 days of the growth of the film (with *in situ* nitrogen annealing). Au/In contacts were used as electrodes. The inset shows the *I-V* characteristics for (ZnAs)O film just after the growth with *in situ* rapid thermal annealing at 200 °C in nitrogen.

vacancies is suppressed by doping with Mn. However, the MIT in both films may be explained due to the percolation of charge carriers, probably due to the competition between the semiconducting (or insulating) and the metallic (due to oxygen vacancy and As doping) behaviors in the film. That is also reflected from the weak MIT peak in (ZnAs)MnO, in which Mn reduces the metallic percolation due to the reduction of ionization efficiency on oxygen vacancies.

In order to study the annealing and aging effects, room-temperature current-voltage (*I-V*) of these films were determined and presented in Fig. 4. It is noted that either In or In/Au contacts hardly affected the transport results. All the contacts made on the film exhibit a linear *I-V* behavior, indicating an Ohmic contact. The resistivity of (ZnAs)O films measured within a week of their fabrication was in the range of 2–3 Ω cm, and a typical *I-V* curve for (ZnAs)O film is shown in the inset of Fig. 4. However, the resistivity increased very fast with time in both films, reaching about 4 KΩ cm. Furthermore, rapid thermal annealing in nitrogen for 3 min changed the resistivity to 2 KΩ cm. However, successive annealing in nitrogen hardly changes the resistivity value in (ZnAs)O, as shown in Fig. 4. Similar trend was also observed for (ZnAs)MnO film. Unlike the metallic conductivity observed in Al and Ga doped in ZnO, the electrical conductivity observed in As-doped ZnO is not stable. Most probably, the oxygen vacancies, which are mainly responsible for conduction, are reduced faster in As-doped ZnO films on aging than other doping, such as Ga or Al. Hence, it is suggested that As may not be a good doping candidate for achieving higher metallic conductivity in ZnO films.

In summary, we have synthesized As-doped ZnO and Mn-doped (ZnAs)O films using pulsed-laser deposition technique. The x-ray diffraction studies show that the films are *c*-axis oriented and crystalline in nature. The grain size in (ZnAs)O decreases from 40 to less than 10 nm in Mn doping, indicating that Mn acts as catalyst apart from dopant. Temperature dependent electrical resistance shows metal-insulator and metal-semiconductor transitions at 165 and 115 K, respectively, in (ZnAs)O film. The observation of MIT and MST at low temperatures in ZnO due to arsenic doping are certainly intriguing and further work is needed to understand these phenomena. Although doping with Mn suppresses MST completely, a weak peak is seen for MIT. Both ionization efficiency on oxygen vacancies and percolation of charge carriers may be responsible for such transitions. In addition, electrical conduction in these films shows strong aging effects, suggesting that As is not an ideal dopant for higher conductivity in ZnO films.

This work is supported by the NASA and NSF for Center for Research Excellence in Science and Technology (CREST) Grant No. HRD-9805059.

[1]T. Soki, Y. Hatanaka, and D. C. Look, Appl. Phys. Lett. **76**, 3257 (2000).
[2]K. Minegishi, Y. Koiwai, Y. Kikuchi, K. Yano, M. Kasuga, and A. Shimizu, Jpn. J. Appl. Phys., Part 2 **36**, L1453 (1997).
[3]Y. Yan, S. B. Zhang, and S. T. Pantelides, Phys. Rev. Lett. **86**, 5723 (2001).
[4]E.-C. Lee, Y. S. Kim, Y. G. Jin, and K. J. Chang, Phys. Rev. B **64**, 085120 (2001).
[5]D. C. Look, D. C. Reynolds, C. W. Litton, R. L. Jones, D. B. Eason, and G. Cantwell, Appl. Phys. Lett. **81**, 1830 (2002).
[6]K.-K. Kim, H.-S. Kim, D.-K. Kwang, J.-H. Lim, and S.-J. Park, Appl. Phys. Lett. **83**, 63 (2003).
[7]Y. R. Ryu, T. S. Lee, J. H. Lee, and H. W. White, Appl. Phys. Lett. **83**, 4032 (2003).
[8]V. Vaithianathan, B.-T. Lee, and S. S. Kim, Appl. Phys. Lett. **86**, 062101 (2005).
[9]N. F. Mott, *Metal-Insulator Transition* (Taylor & Francis, London, 1974).
[10]V. Bhosle, A. Tiwari, and J. Narayan, Appl. Phys. Lett. **88**, 032106 (2006).
[11]Y. Furubayashi, T. Hitosugi, Y. Yamamoto, K. Inaba, G. Kinodo, Y. Hirose, T. Shimada, and T. Hasegawa, Appl. Phys. Lett. **86**, 252101 (2005).
[12]R. C. Budhani, P. Pant, R. K. Rakshit, K. Senapati, S. Mandal, N. K. Pandey, and J. Kumar, J. Phys.: Condens. Matter **17**, 75 (2005).